

# History, Science and Materials of RTGs

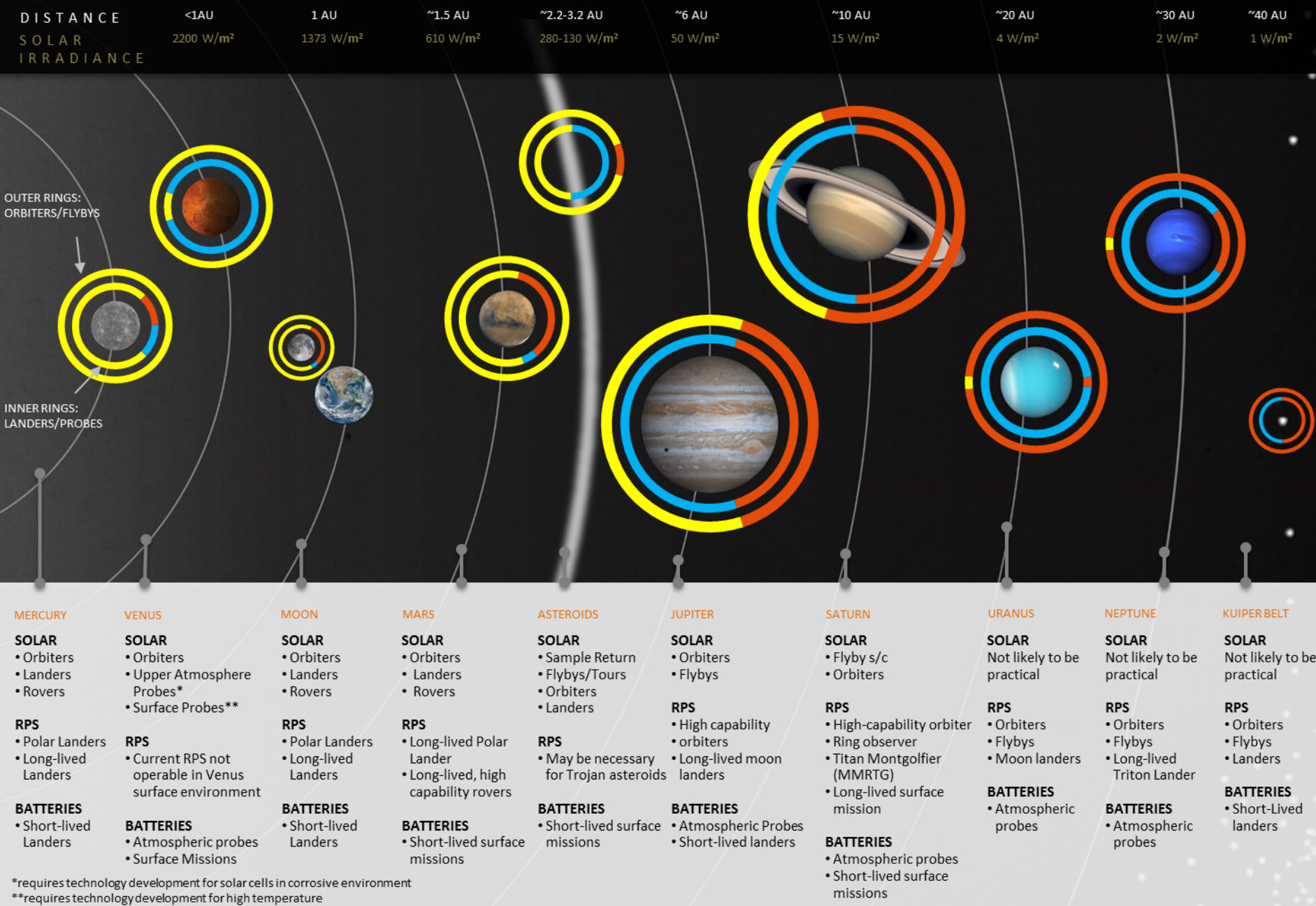
Giacomo Cerretti<sup>1,2</sup>, Sabah K. Bux<sup>2</sup>, Jean-Pierre Felurial<sup>2</sup>

<sup>1</sup>NASA Postdoctoral Program (NPP) fellow.

<sup>2</sup>Power and Sensor Systems Section, NASA Jet Propulsion Laboratory, California Institute of Technology, 4800 Oak Grove Drive, Pasadena, California 91109, USA.

JPL Postdoc Seminar

12/16/2019



\*requires technology development for solar cells in corrosive environment  
 \*\*requires technology development for high temperature

### POWER TECHNOLOGIES APPLICABLE TO SOLAR SYSTEM EXPLORATION MISSION CONCEPTS AS OF 2015<sup>(1)</sup>

(1) Notional mission applicability based on expert opinion developed in JPLA-Team study in August, 2015. Updated 2017.

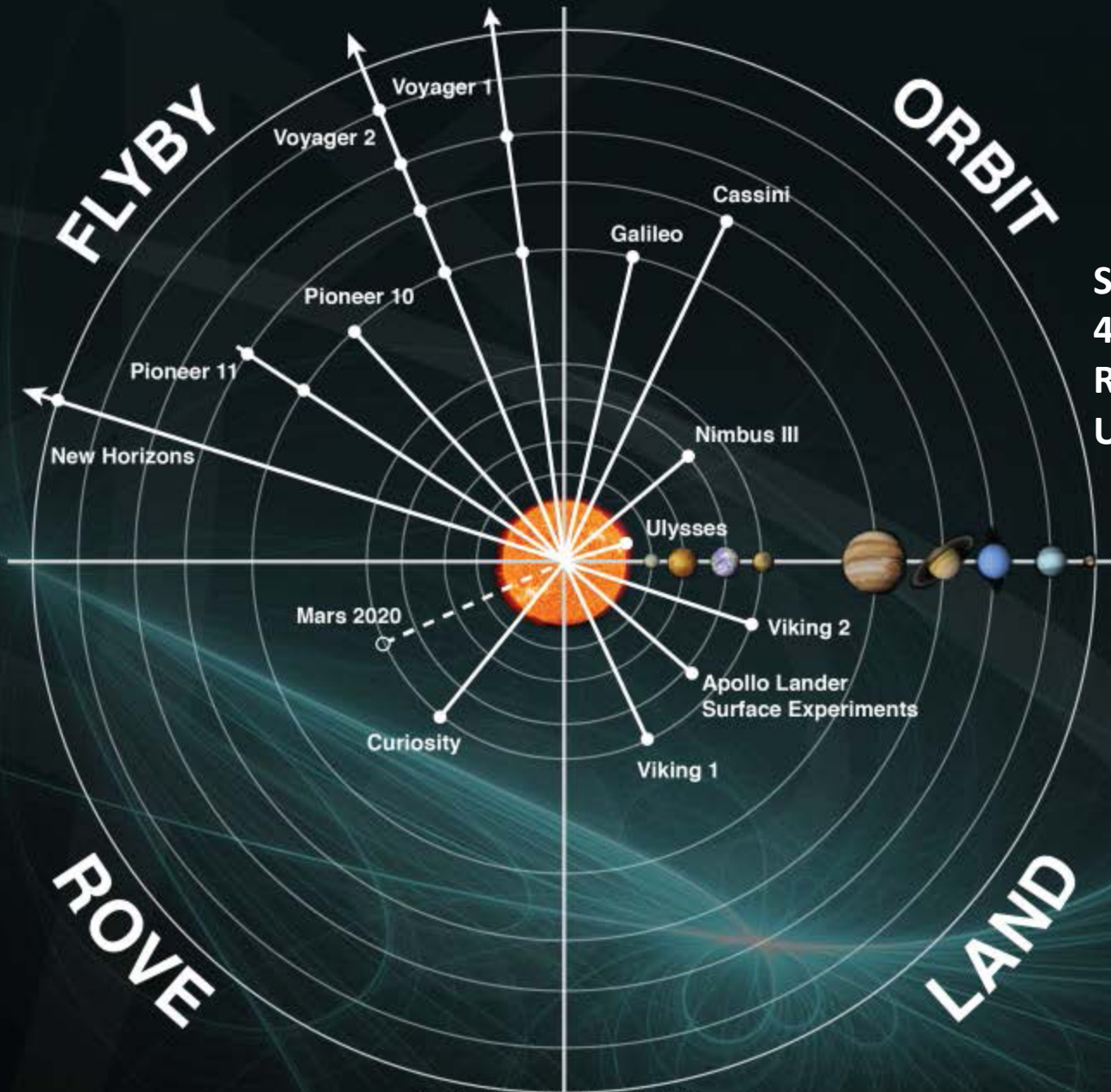
■ Solar  
■ RPS  
■ Primary Battery

*Approximate relative applicability of power technologies to target body missions*

SOLAR PROGRAM  
powered by USA

# Over 50 years of RPS Missions

1961  
1971  
1981  
1991  
2001  
2011  
2021

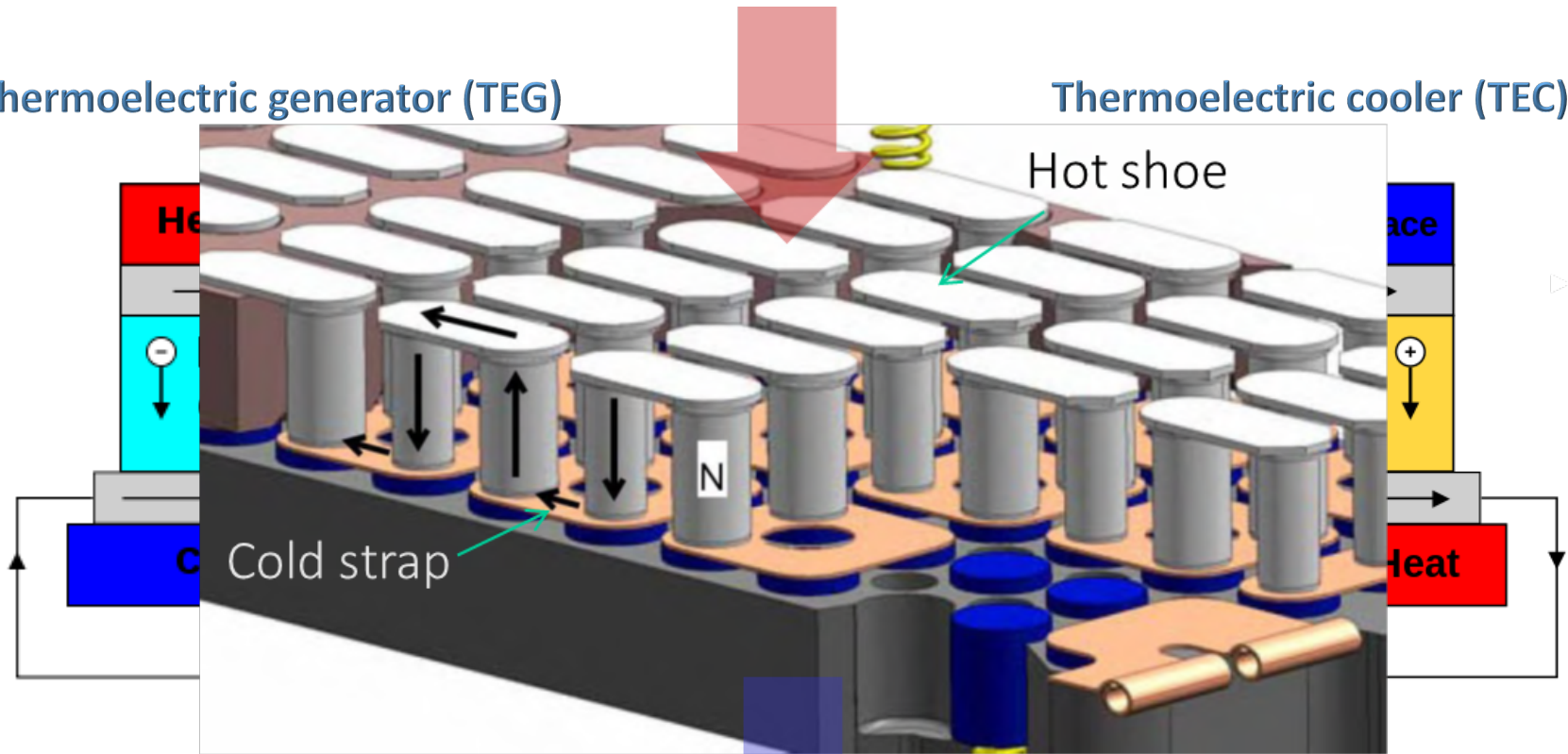


Since 1961:  
46 individual  
RTGs used on 27  
U.S. missions.

# Thermoelectric conversion

Thermoelectric generator (TEG)

Thermoelectric cooler (TEC)



Seebeck effect

Peltier effect

$$\Delta V = S\Delta T$$

$$\dot{Q} = STI = \Pi I$$

# eMMRTG architecture

<https://mars.nasa.gov/resources/6032/panoramic-view-from-west-of-dingo-gap/>

Multi-mission Radioisotope Thermoelectric Generator (MMRTG) on Curiosity

Microth

Thermoelec  
Asser

Modu

K

CO<sub>2</sub>

pellets

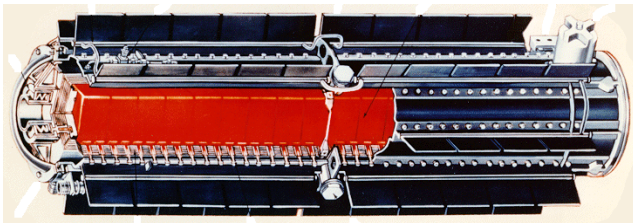
<https://rps.nasa.gov/resources/56/enhanced-multi-mission-radioisotope-thermoelectric-generator-emmrtg-concept/>

# State of the art RTGs materials

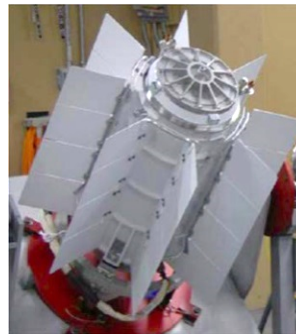
- RTGs for the past 50 years have either been PbTe or SiGe based
  - ~6.5% efficiency at the system level
  - High level of reliability and long life
- Increasing demand for higher RTG conversion efficiency
  - Higher specific power (W/kg) needed for larger scientific payloads
    - Limited amount of expensive heat source

***Need to develop advanced thermoelectric materials***

Mission name	TE Mater.	Launch year
Transit 4A	<b>PbTe</b>	1961
Transit 4B	<b>PbTe</b>	1962
Apollo 12	<b>PbTe</b>	1969
Triad-01-1x	<b>PbTe</b>	1972
Pioneer 10	<b>PbTe</b>	1972
Pioneer 11	<b>PbTe</b>	1973
Viking 1	<b>PbTe</b>	1975
Viking 2	<b>PbTe</b>	1975
LES 8	<b>Si-Ge</b>	1976
LES 9	<b>Si-Ge</b>	1976
Voyager 1	<b>Si-Ge</b>	1977
Voyager 2	<b>Si-Ge</b>	1977
Galileo	<b>Si-Ge</b>	1989
Ulysses	<b>Si-Ge</b>	1990
Cassini	<b>Si-Ge</b>	1997
New Horizons	<b>Si-Ge</b>	2006
MSL	<b>PbTe</b>	2011



SiGe GPHS RTG (1980-2006)



PbTe/TAGS MMRTG (2008-present)

# Thermoelectric power generation

## Efficiency

$$\eta_{\max} = \frac{\overset{\text{Carnot}}{T_{\text{hot}} - T_{\text{cold}}}}{T_{\text{hot}}} \frac{\overset{\text{TE Materials}}{\sqrt{1 + ZT} - 1}}{\sqrt{1 + ZT} + \frac{T_{\text{cold}}}{T_{\text{hot}}}}$$

## Figure of merit

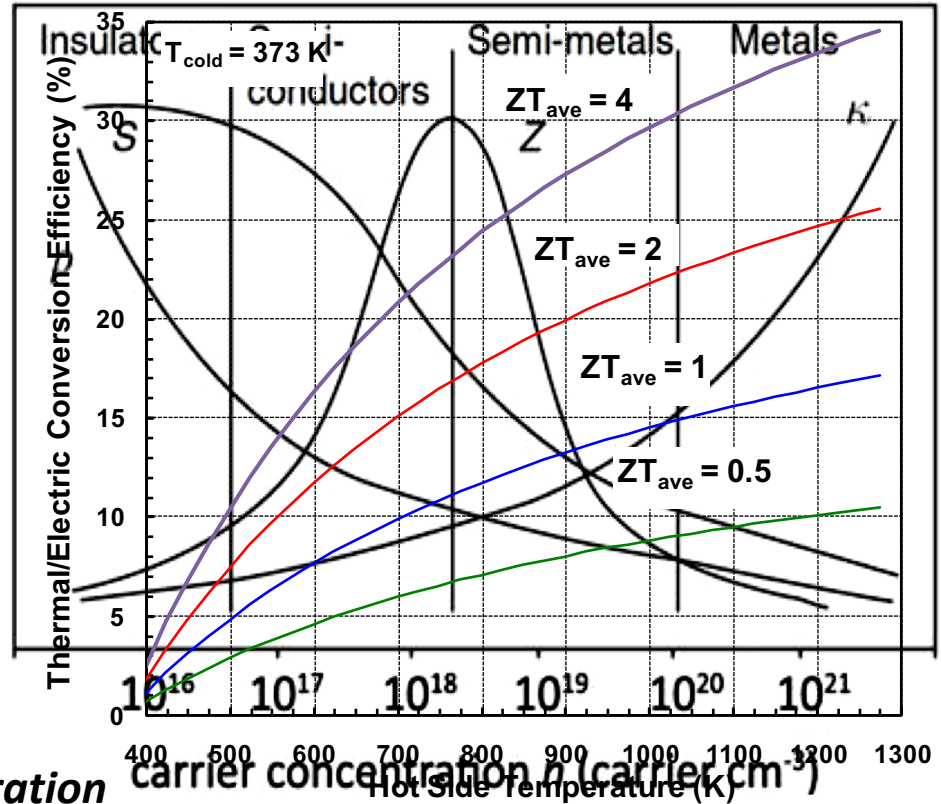
$$zT = \frac{S^2 T}{\rho \kappa}$$

$S$  = Seebeck coefficient  
(thermopower)

$\rho$  = Electrical resistivity

$\kappa$  = Thermal conductivity

$T$  = Absolute temperature



## Power generation

(across 1275 to 300 K)

State-Of-Practice materials:

Challenge: Decouple the electronic and thermal transport

State-Of-the-Art materials:

$ZT_{\text{average}} \sim 0.5$   
 $ZT_{\text{average}} \sim 1.1$  "phonon glass, electron crystal"

Best SOA materials:

$ZT_{\text{peak}} \sim 1.5$  to  $2.0$

# Fundamental equations

$$zT = \frac{S^2 T}{\rho \kappa}$$

## Electronic transport

$$\sigma = \frac{1}{\rho} = n \cdot e \cdot \mu = n \cdot e^2 \cdot \frac{\tau}{m^*}$$

$$S = \frac{8m^* \pi^2 k_B^2}{3e\hbar} T \left( \frac{\pi}{3n} \right)^{\frac{2}{3}}$$

$n$  = charge carrier concentration

$\mu$  = charge carrier mobility

$e$  = elementary charge

$m^*$  = cc effective mass

$\tau$  = relaxation time

$k_B$  = Boltzmann const.

$\hbar$  = Planck's const.

$L$  = Lorenz number

$C_p$  = heat capacity

$v_g$  = phonon velocity

$\Lambda$  = phonon mean free path

## Thermal transport

$$\kappa = \kappa_{el} + \kappa_L$$

$$\kappa_{el} = L \cdot \sigma \cdot T$$

$$\kappa_L = \frac{1}{3} C_p \cdot v_g \cdot \Lambda$$



# Technical approach to materials

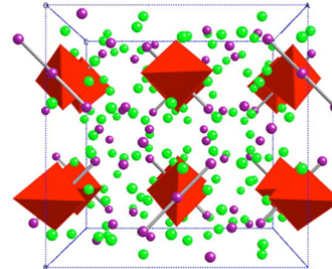
Need for high performance materials that are chemically, thermally, and mechanically stable across wide  $\Delta T$ .

## ***Approach 1: Complex crystal structures***

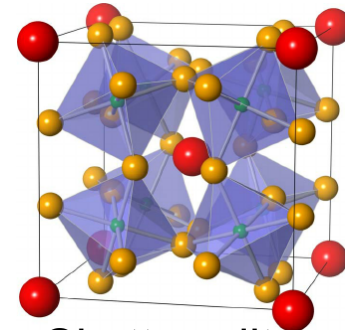
- Inherently low thermal conductivity
- Optimization electronic transport properties

### ***Challenges:***

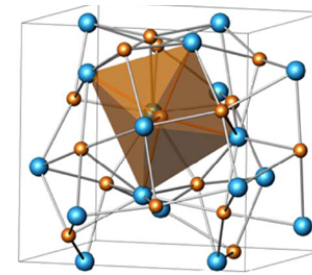
- Find synthetic methods that enable precise stoichiometric control and practical scaling up
- Having theoretical guidance to predict structure-properties relations



Zintl phases



Skutterudites



$\text{Th}_3\text{P}_4$

## ***Approach 2: Introducing nano features in already known good semiconductors***

- Reduce thermal conductivity and improve electronic properties via compositing nanoscale grains within bulk materials

### ***Challenges:***

- Precise control over size, distribution, and composition of nano inclusions
- Retaining nanoscale features even after consolidation in bulk pellets

# Optimization strategies

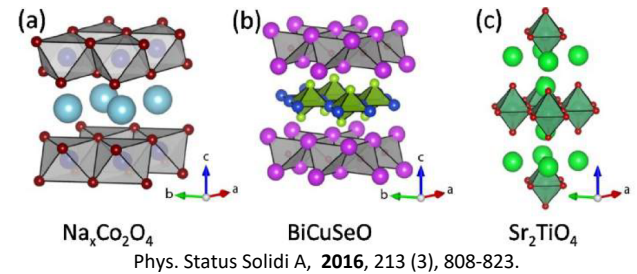
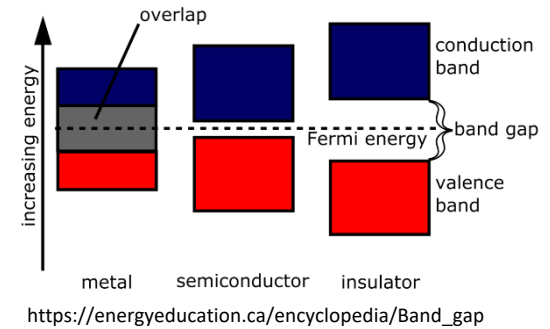
## Improving electronic properties:

- **Doping/Alloying**

- Manipulation of  $n$ .
- Band engineering ( $E_F$ ,  $E_g$ , *degeneracy*,  $m^*$ ,  $\mu$ ).

- **Modulation:**

- Layered or complex structures. E.g. superlattices, layered cobaltites ( $\text{Na}_x\text{Co}_2\text{O}_4$ ), oxyselenides ( $\text{BiCuSeO}$ ), Ruddlesden-Popper phases ( $\text{Sr}_2\text{TiO}_4$ ).



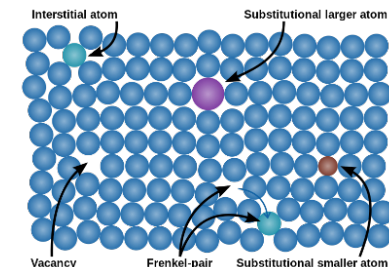
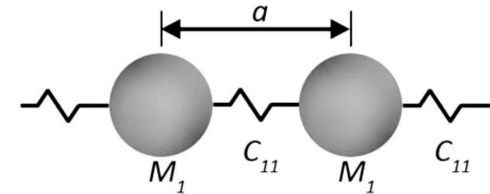
## Improving thermal properties:

- **Doping/Alloying**

- Changes in bond character (ionicity, covalency) length, strength.
- Changes in mass and size of ions.

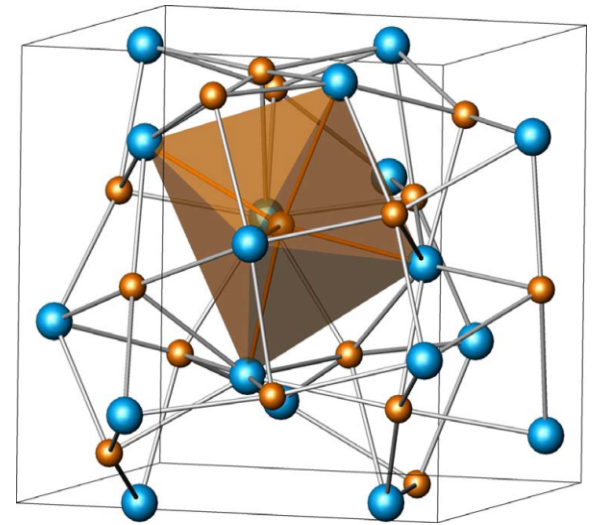
- **Nanostructuring**

- **Defects** (point defects, vacancies, CS planes)

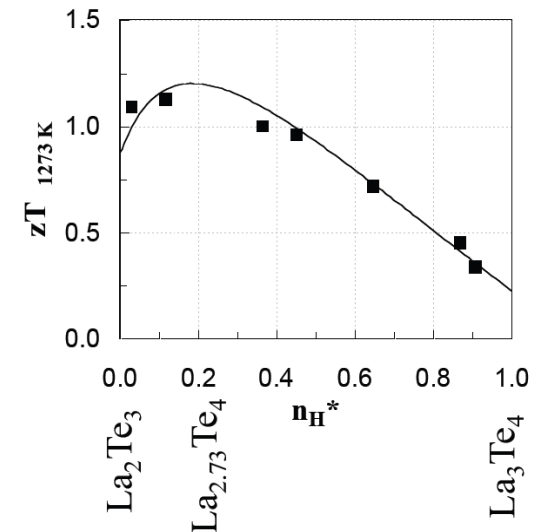


# n-type $\text{La}_{3-x}\text{Te}_4$

- **Known good TE materials since the 1970's**
- **Complex crystal structure**
  - Defect  $\text{Th}_3\text{P}_4$  structure-type (I-43d)  
28 atoms per unit cell  
up to 1/9 of La positions can be vacant
- **Low thermal conductivity** ( $\sim 2 \text{ Wm}^{-1}\text{K}^{-1}$ )
- **Good electrical properties**
  - Controlled by vacancy concentration on La site
- **Difficult to synthesize**  
Multi-step high temperature processes  $\rightarrow$  low reproducibility of electronic properties
- **New synthesis developed at JPL**  
Powder metallurgy synthesis method, enabling reproducible optimization of TE properties
- **Peak  $zT_{1273 \text{ K}} \approx 1.2$**

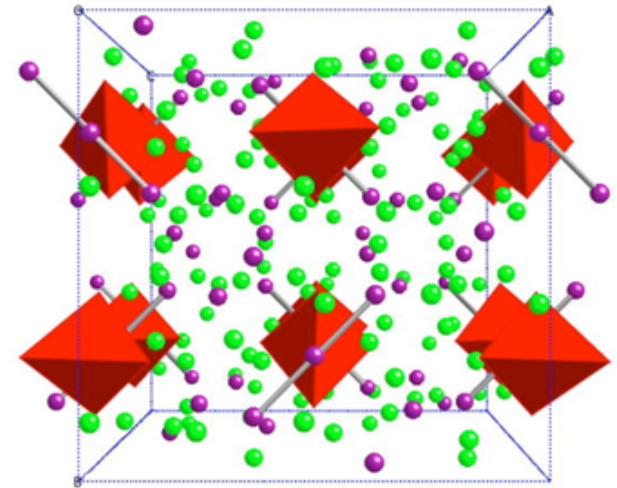


Fully filled crystal structure of  $\text{La}_3\text{Te}_4$

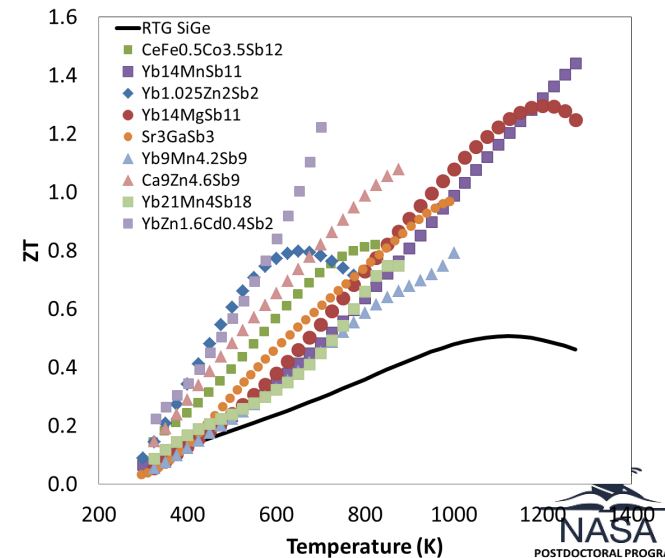


# p-type $\text{Yb}_{14}\text{MnSb}_{11}$

- $\text{Yb}_{14}\text{MnSb}_{11}$ 
  - Zintl Structures
  - Covalent, anionic substructures:  $[\text{MPn}_4]^{9-}$ ,  $[\text{Pn}_3]^{7-}$ ,  $4\text{Pn}^{3-}$ ,  $14\text{A}^{2+}$
  - Zintl-Klemm valence count: essentially complete electron transfer between cation and anion
  - Body centered tetragonal ( $I4_1/acd$ )
  - 208 atoms per unit cell
- **Low thermal conductivity** ( $\sim 0.85 \text{ Wm}^{-1}\text{K}^{-1}$ )
- **Tunable electronic properties via doping**
- **Peak  $zT \sim 1.3$  @  $1273\text{K}$**
- **Factor of 3x over SiGe**



$\text{Yb}_{14}\text{MnSb}_{11}$



# p-type material optimization

**$\text{Yb}_{14}\text{MnSb}_{11}$  composites**

# Composite metal (M) choice



Inclusions	M-Sb Reactivity	$\rho$ [n $\Omega$ ·m] @25°C	E [GPa]	CTE [um/mK] @25°C
Ni	High	69.3	200	13.4
Co	Low	62.4	209	13

- Ni reacted with matrix forming secondary phases → not good.

- We used Co →



**Cobalt Composite Network Using Thermoelectrics (CoCoNUT)**

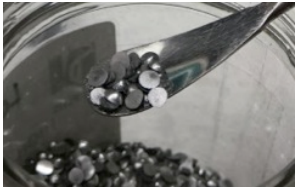
# Yb<sub>14</sub>MnSb<sub>11</sub> + M synthesis

Yb<sub>14</sub>MnSb<sub>11</sub>

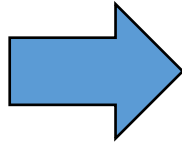
+2vol%Co (W)

+5vol%Co (W)

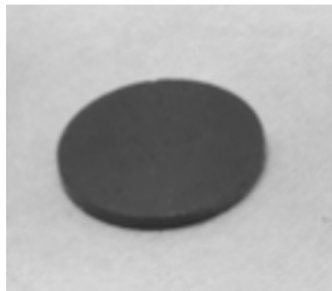
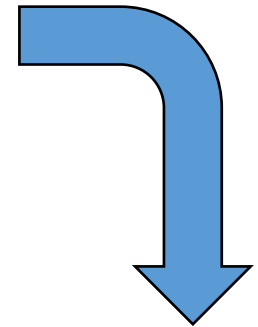
+10vol%Co



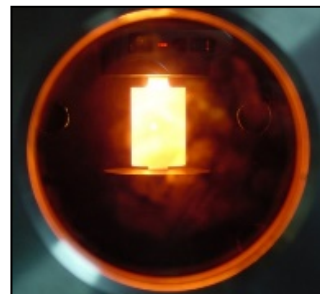
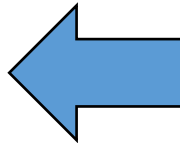
Mix precursors  
(Yb, MnSb, Sb +  
CoSb/W)



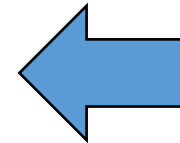
High energy ball mill



1/2" pellets  
>98% density

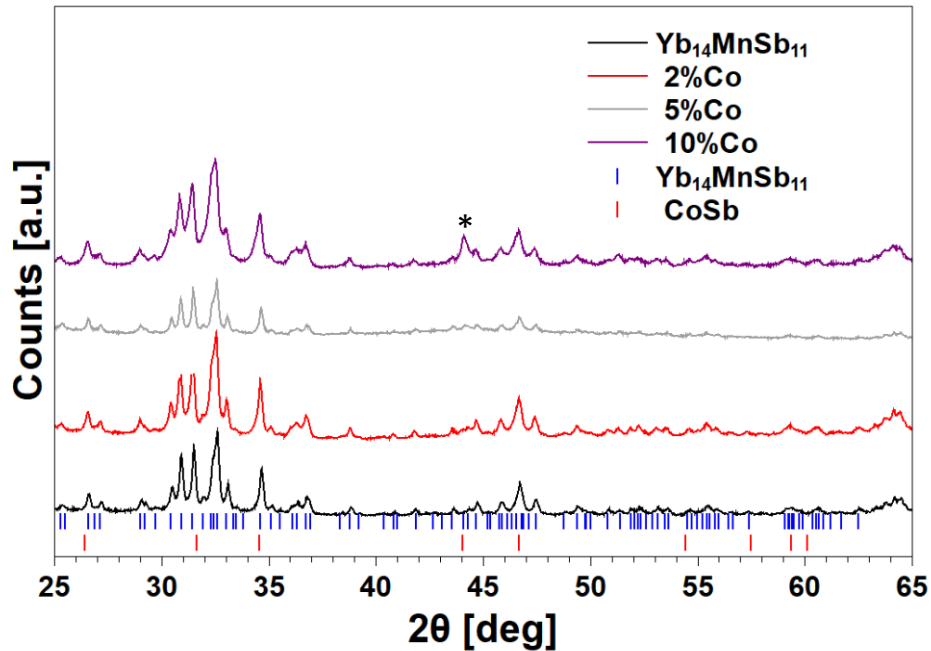


SPS  
Synthesis/compaction

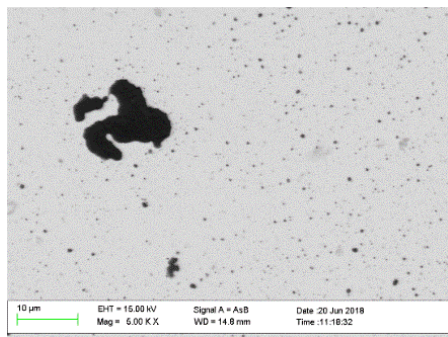


Homogenized  
powder

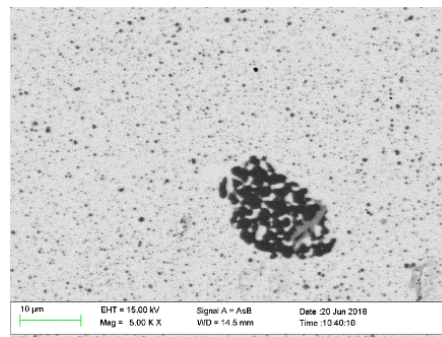
# Co Compositing in $\text{Yb}_{14}\text{MnSb}_{11}$



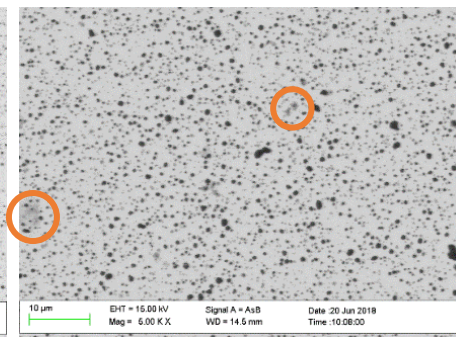
- Profile of each sample matches with  $\text{Yb}_{14}\text{MnSb}_{11}$ .
- Sample with 10%Co shows CoSb Impurities.
- Inclusions sizes between nm and several  $\mu\text{m}$ .
- Signs of CoSb in 10%Co sample.



2vol%

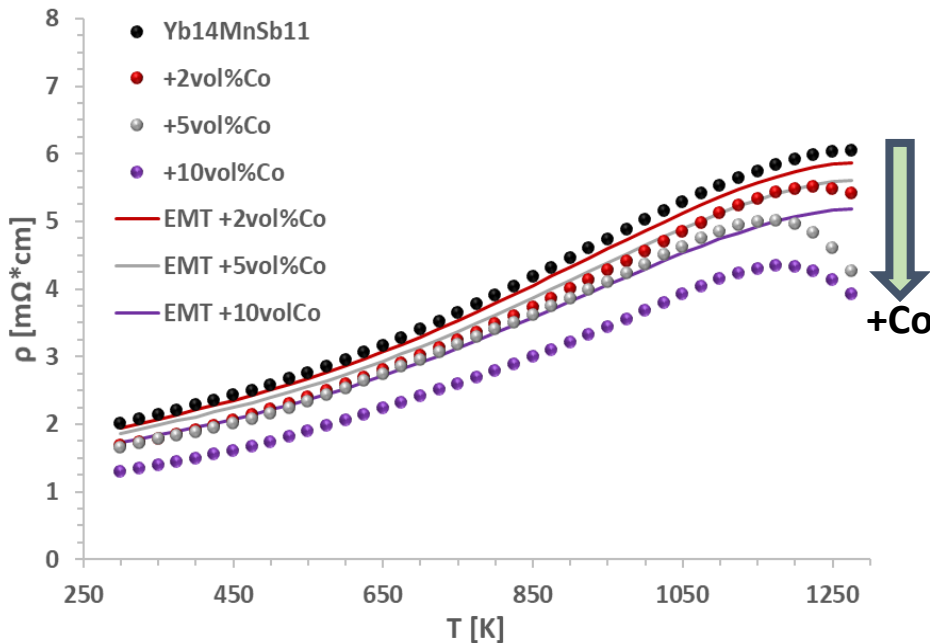


5vol%



10vol%

# Co Compositing in $\text{Yb}_{14}\text{MnSb}_{11}$



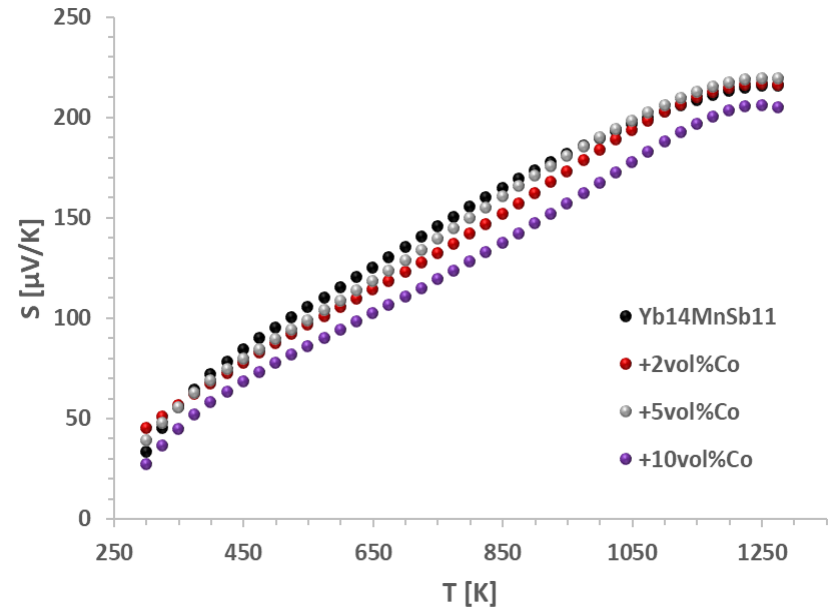
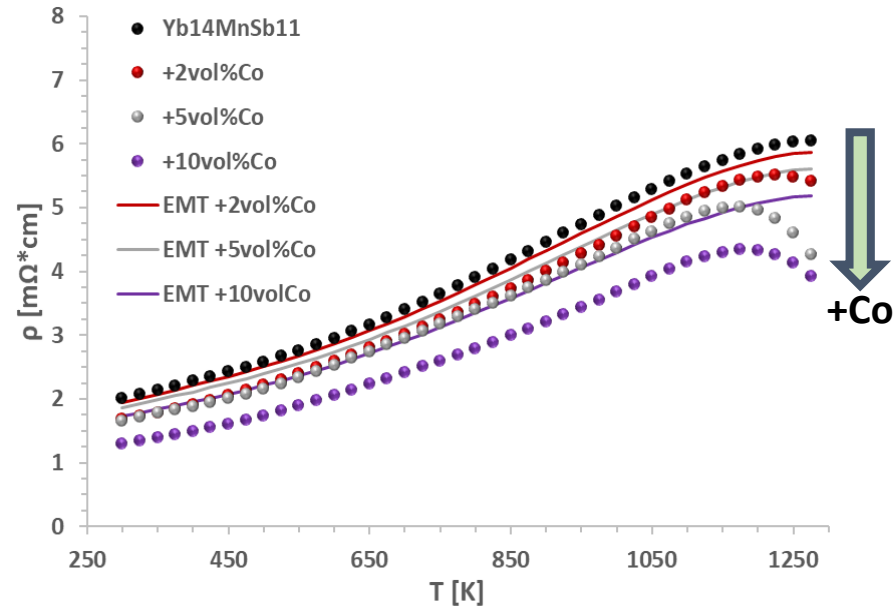
- More M  $\rightarrow$  more conductive  $\rightarrow \rho$  decreases (as expected).
- Deviation from EMT increases with higher inclusions content  $\rightarrow$  model is missing something.

EMT

K = conductivity (resistivity)  
 1 = matrix  
 2 = inclusion  
 v = volume fraction

$$K = \frac{k_1 v_1 + k_2 v_2 \frac{3k_1}{2k_1 + k_2}}{v_1 + v_2 \frac{3k_1}{2k_1 + k_2}}$$

# Co Compositing in $\text{Yb}_{14}\text{MnSb}_{11}$



- More M  $\rightarrow$  more conductive  $\rightarrow \rho$  decreases (as expected).
- Despite reduction in  $\rho$ , the Seebeck remains constant.

$$\sigma = \frac{1}{\rho} = n \cdot e \cdot \mu = n \cdot e^2 \cdot \frac{\tau}{m^*}$$

$$S = \frac{8m^* \pi^2 k_B^2}{3e\hbar} T \left( \frac{\pi}{3n} \right)^{\frac{2}{3}}$$

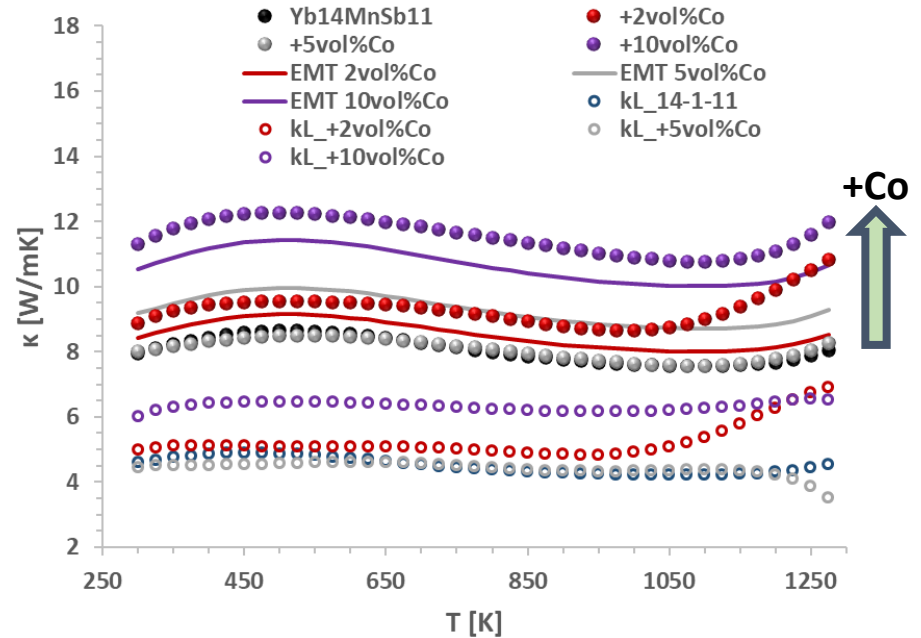
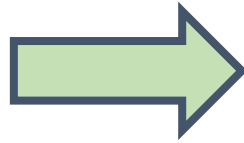
# Co Compositing in $\text{Yb}_{14}\text{MnSb}_{11}$

$$\kappa = 1000 \cdot C_p \cdot d \cdot D \left[ \frac{W}{m \cdot K} \right]$$

$C_p$  = heat capacity [J/(g\*K)]

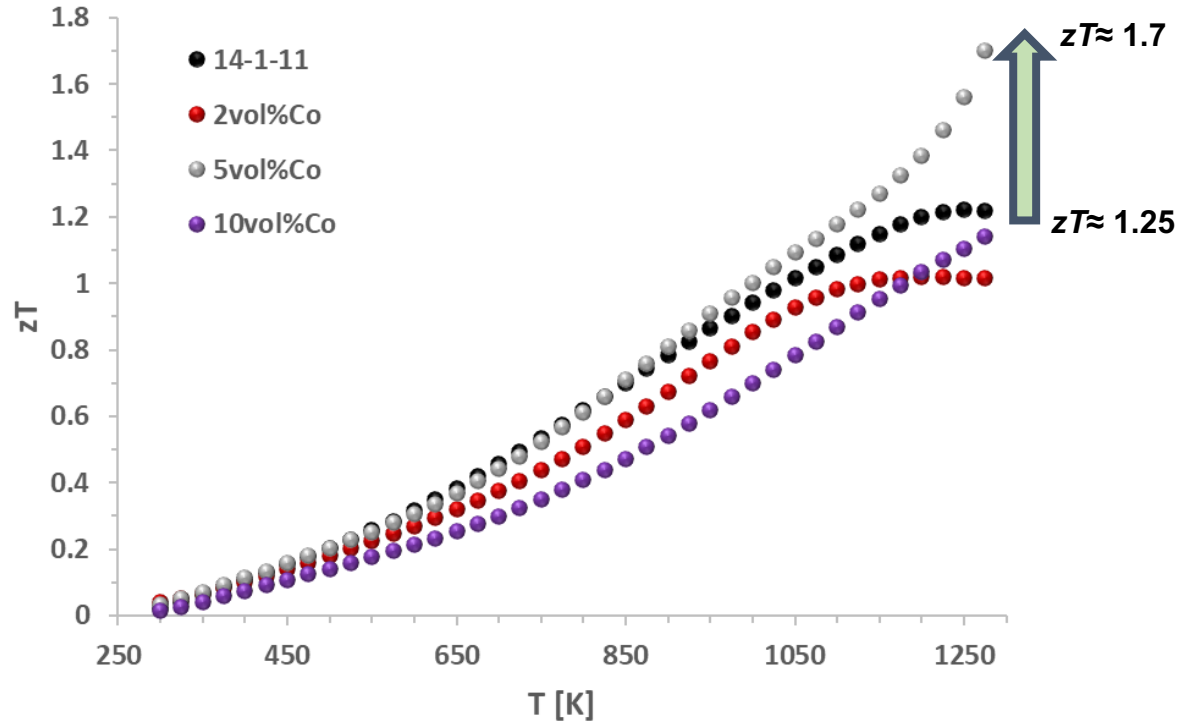
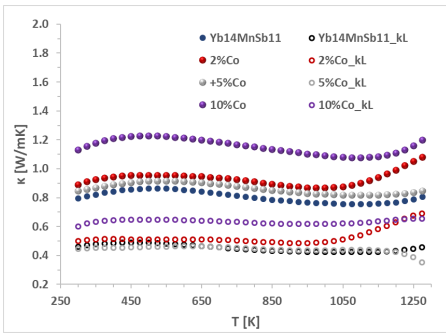
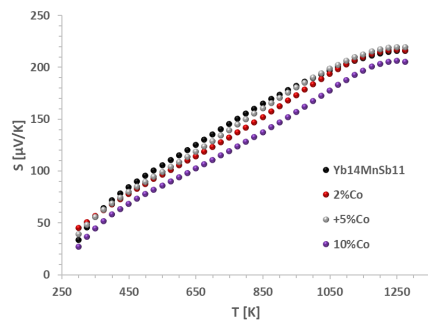
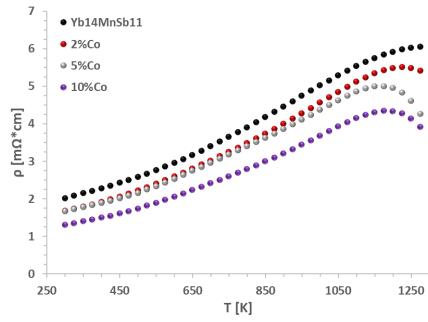
$d$  = density [g/cm<sup>3</sup>]

$D$  = diffusivity [cm<sup>2</sup>/s]



- Lattice contributions to thermal conductivity derived from Wiedemann-Franz law ( $\kappa_L = \kappa - L\sigma T$ ).
- $C_p$  corrected to include contribution from Co.
- The sample with 10vol% inclusions pays penalties on  $zT$  due to increased thermal conductivity.

# Thermoelectric performance



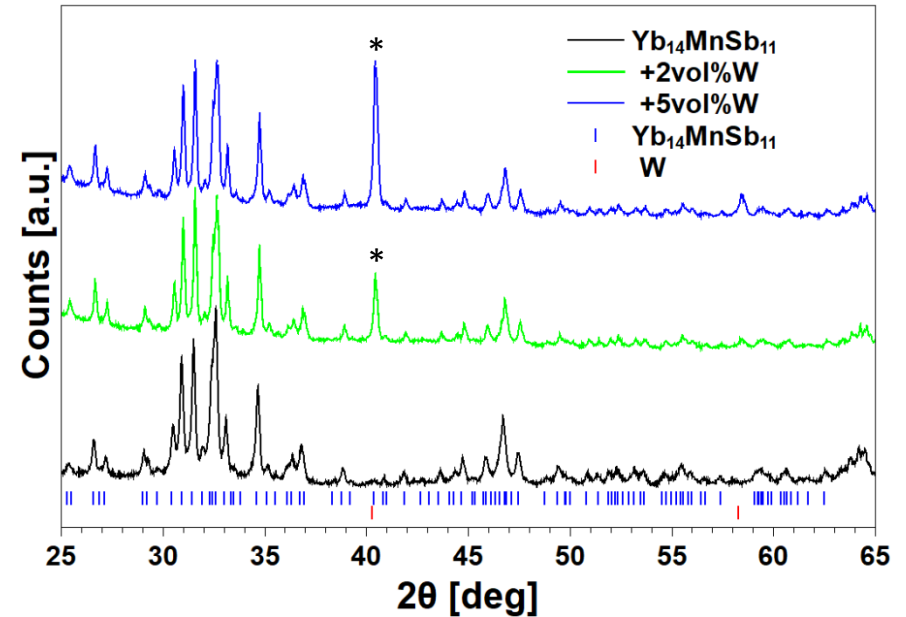
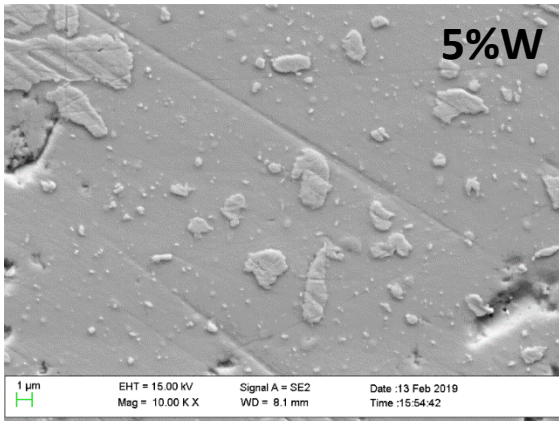
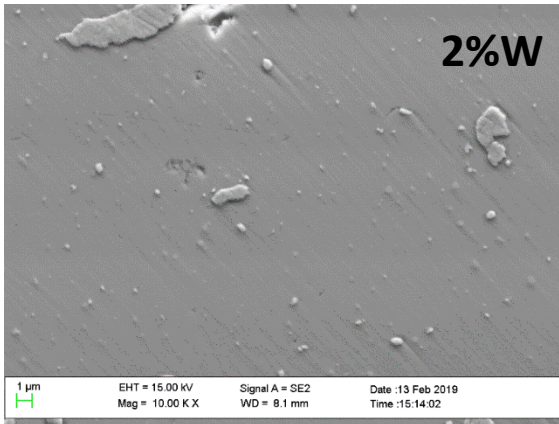
- 5vol% has improved  $zT$  ( $\approx 1.7$  @1273K), due to better electrical ad similar thermal properties.
- Still to understand the transport mechanism to be able to apply it consistently to other material systems.

# Optimization with W composite

Inclusions	M-Sb Reactivity	$\rho$ [n $\Omega$ ·m] @25°C	E [GPa]	CTE [um/mK] @25°C
Ni	High	69.3	200	13.4
Co	Low	64.4	209	13
W	None	52.8	411	4.5

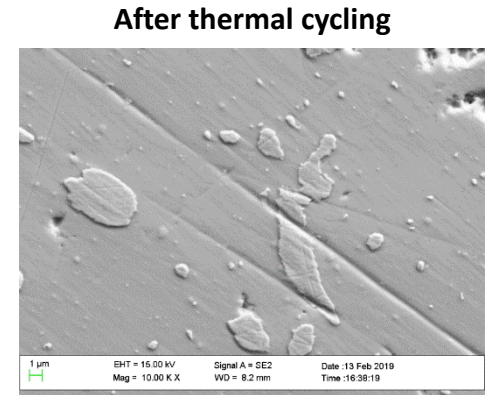
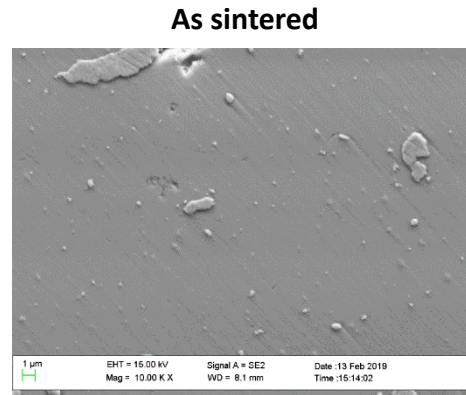
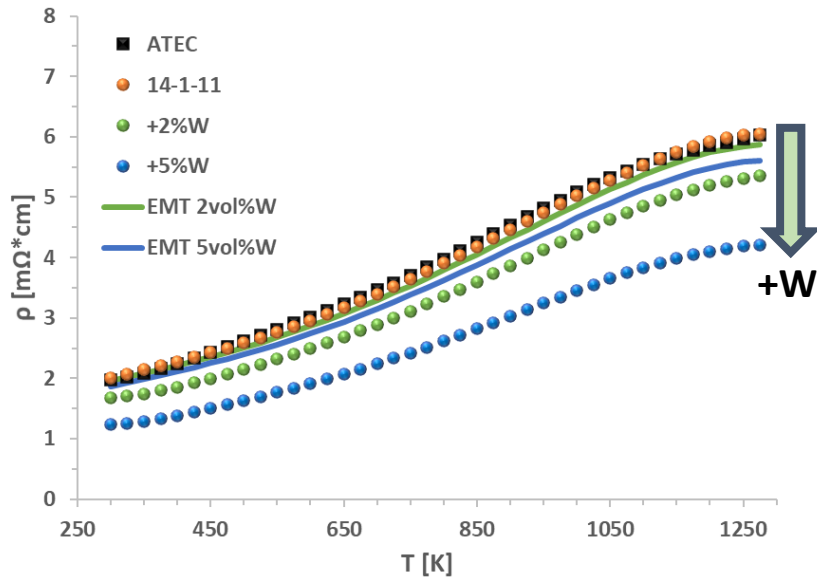
- Lower electrical resistivity compared to previous studies  $\rightarrow$  lower amount will have same effect?
- W does not react with Sb.
- Higher Young's modulus  $\rightarrow$  confer better robustness to composite.
- Lower CTE could generate mechanical instability (cracks) after thermal cycling at the interface inclusion-matrix.

# XRD analysis – microstructure

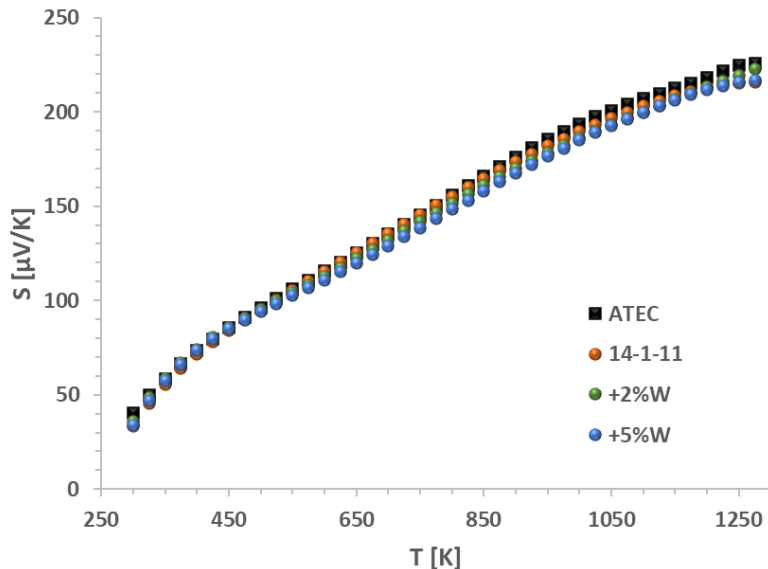


- Profile of each sample matches with  $\text{Yb}_{14}\text{MnSb}_{11}$ .
- W reflections are visible in 2vo%, 5vol% W samples.
- W composite samples show no side phases.
- No cracks radiating from inclusions (CTE mismatch).

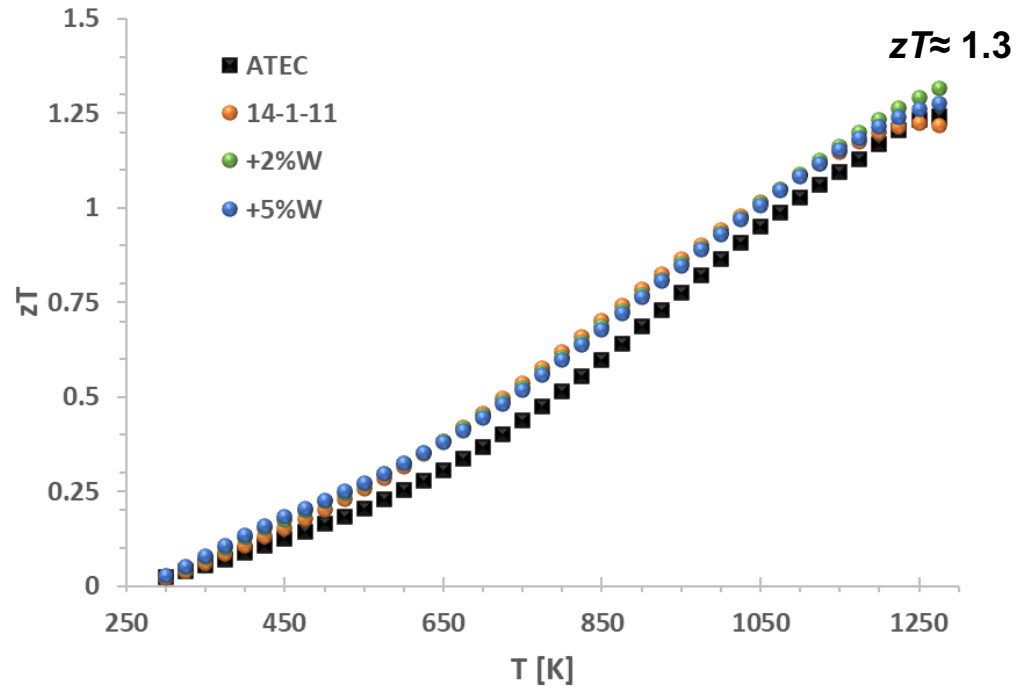
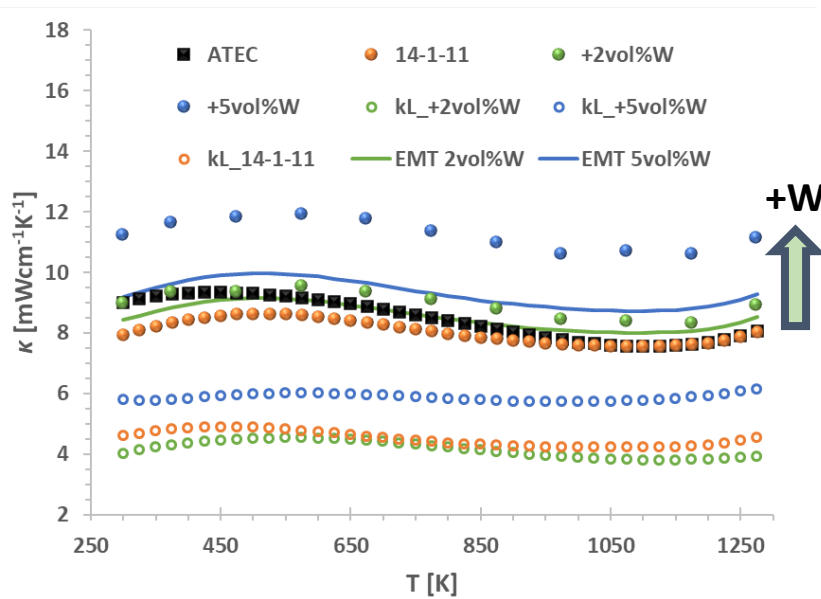
# Electronic transport



- Electrical resistivity substantially decreases at lower inclusion concentrations.
- Comparison with EMT (Maxwell-Euken) shows lower values than predictions.
- Although samples are more conductive, Seebeck remains the same.
- SEM analysis shows no sign of crack generation even after several thermal cycles up to 1273K.

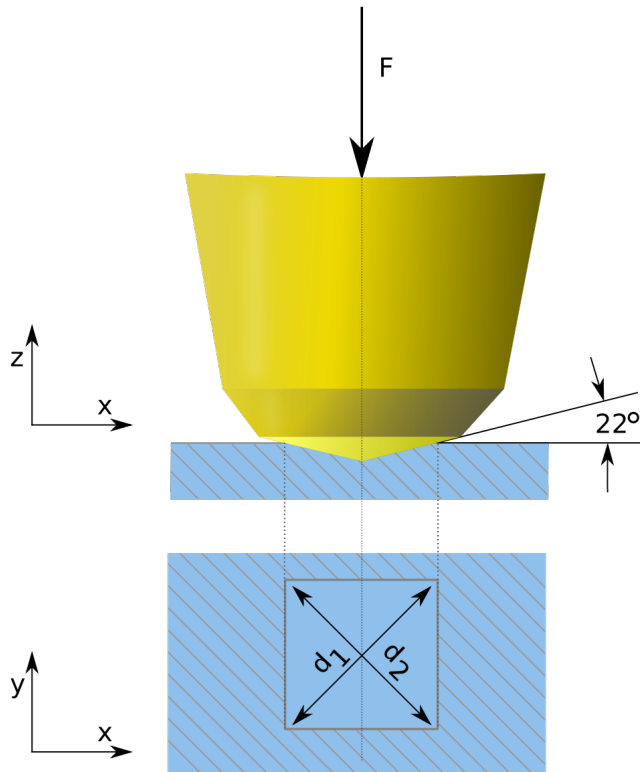


# Thermal transport and zT



- Similarly to Co,  $\kappa_L$  is higher.
- Significant deviation from predicted values (EMT).
- Better electronic properties are washed out by worsening of the thermal conductivity, hence peak  $zT$  remains  $\approx 1.3$  @1273K.

# Vickers Hardness



<https://commons.wikimedia.org/wiki/File:Vickers-path.svg>

Hardness test specifications:

- Diamond indenter
- Loads: 0.01, 0.02, 0.05, 0.1, 0.2, 0.3, 0.5, 1 Kgf
- Indentation time: 10s
- Indentations #: 5 per load

**xxxHVyy/zz**

xxx= hardness number

HV= Hardness Vickers

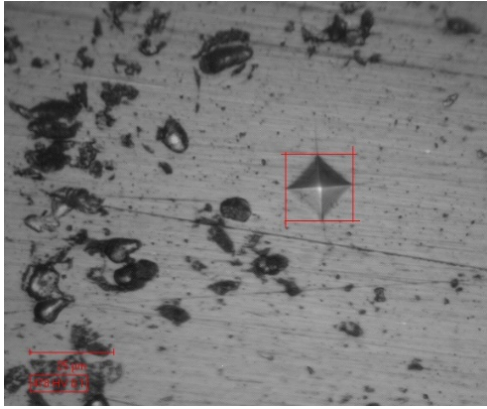
yy= used load in Kgf

zz= loading time if different from 10s or 15s

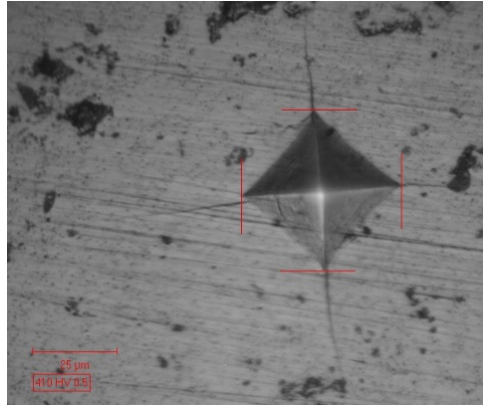
$$HV = \frac{F}{A} = \frac{1.8544F}{d^2} \quad \left[ \frac{Kgf}{mm^2} \right]$$

In good indentations (no tilt of the head and flat sample):  $d = d_1 = d_2$

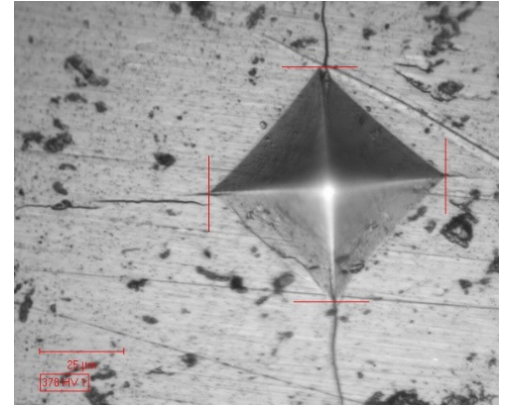
100g



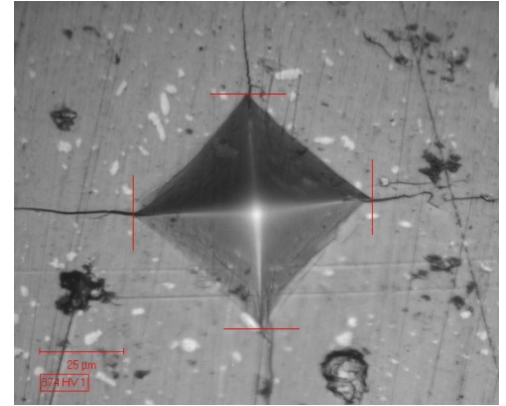
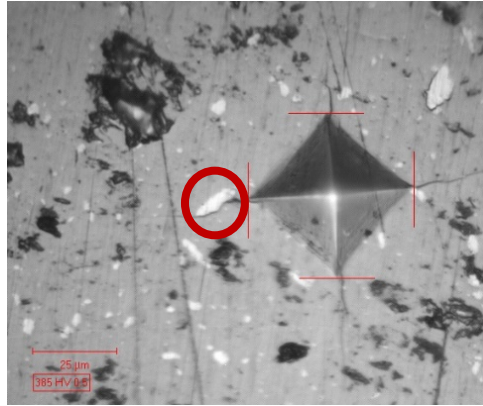
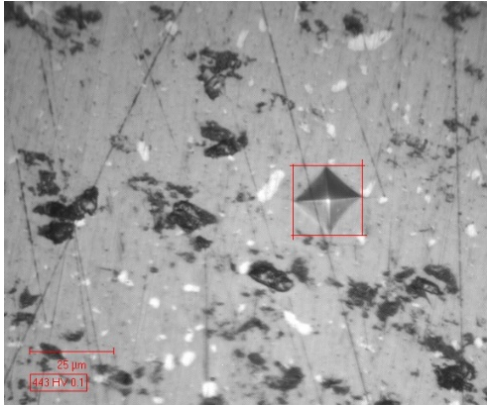
500g



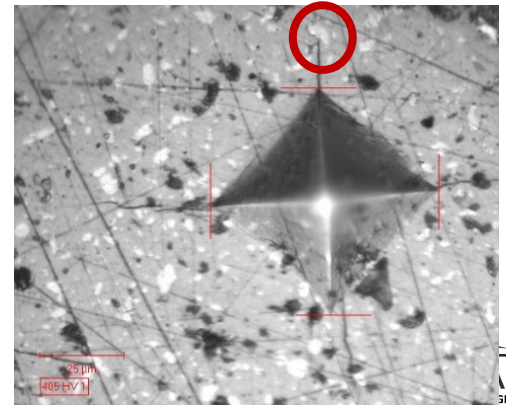
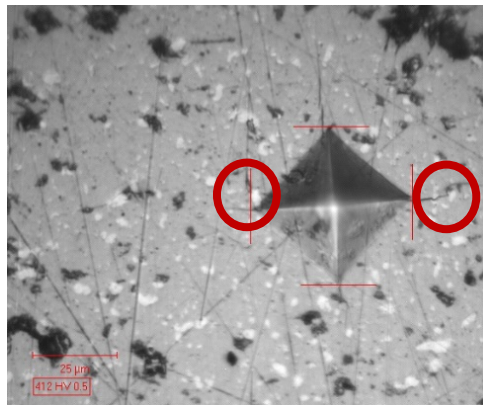
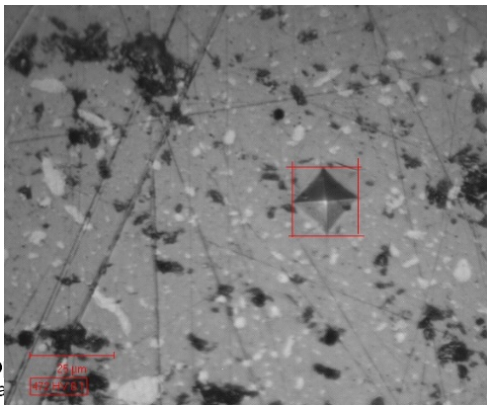
1Kg



14-1-11

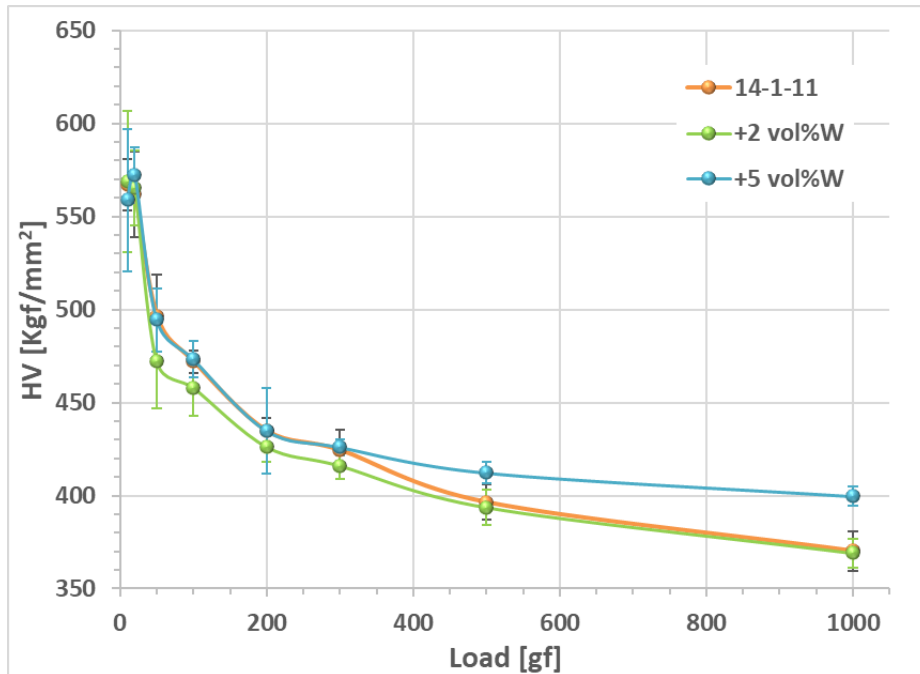


2vol% W



5vol% W

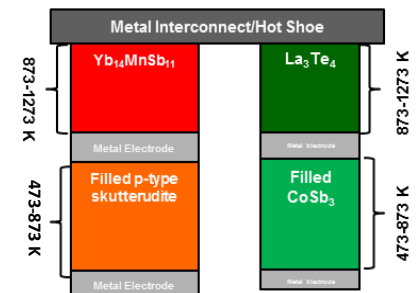
# Hardness of W composite



- At low loads (up to 300gf) the HV values are comparable for all samples.
- At higher loads (0.5 and 1 Kgf) the sample with 5 vol%W shows higher HV.
- Higher HV values and active role in preventing crack propagation confirm the increased mechanical stability of W composite.
- Although thermoelectric performance did not increase, the improved mechanical stability is a big plus for system integration.

# Current optimization strategies

- Manipulation of electronic structures of high performance rare earth chalcogenides (RECh) and pnictides (REPN) based materials.
- Compositing to improve mechanical stability and electronic properties.
- Close coupling between theoretical simulations and systematic experimental research:
  - Computational work to guide experiments.
  - Semi-empirical modeling to optimize materials systems.
- Segmentation:
  - Using segmented legs we can increase the average zT by using materials that have peak zT at different temperatures.



Advanced Segmented Couple  
1273-473 K

# Summary

- RTGs are often the best option to power spacecraft for deep space exploration, due to high reliability, long life, and predictable behavior (power output).
- Modern thermoelectrics can achieve attractive conversion efficiencies:
  - Current device level efficiencies are  $\approx 15\%$  in temperature range 473 - 1273 K.
  - This is a 2x improvement over “heritage” device performance.
- Development of efficient thermoelectrics is a challenging materials science task:
  - Only the first step towards practical implementation.
  - Important improving thermal stability and mechanical robustness through chemical tuning and compositing.
- Improved  $zT$  and mechanical stability have been obtained for p-type  $\text{Yb}_{14}\text{MnSb}_{11}$  using compositing (Co, W).
- Achieved results are promising for future implementation.



# Acknowledgments



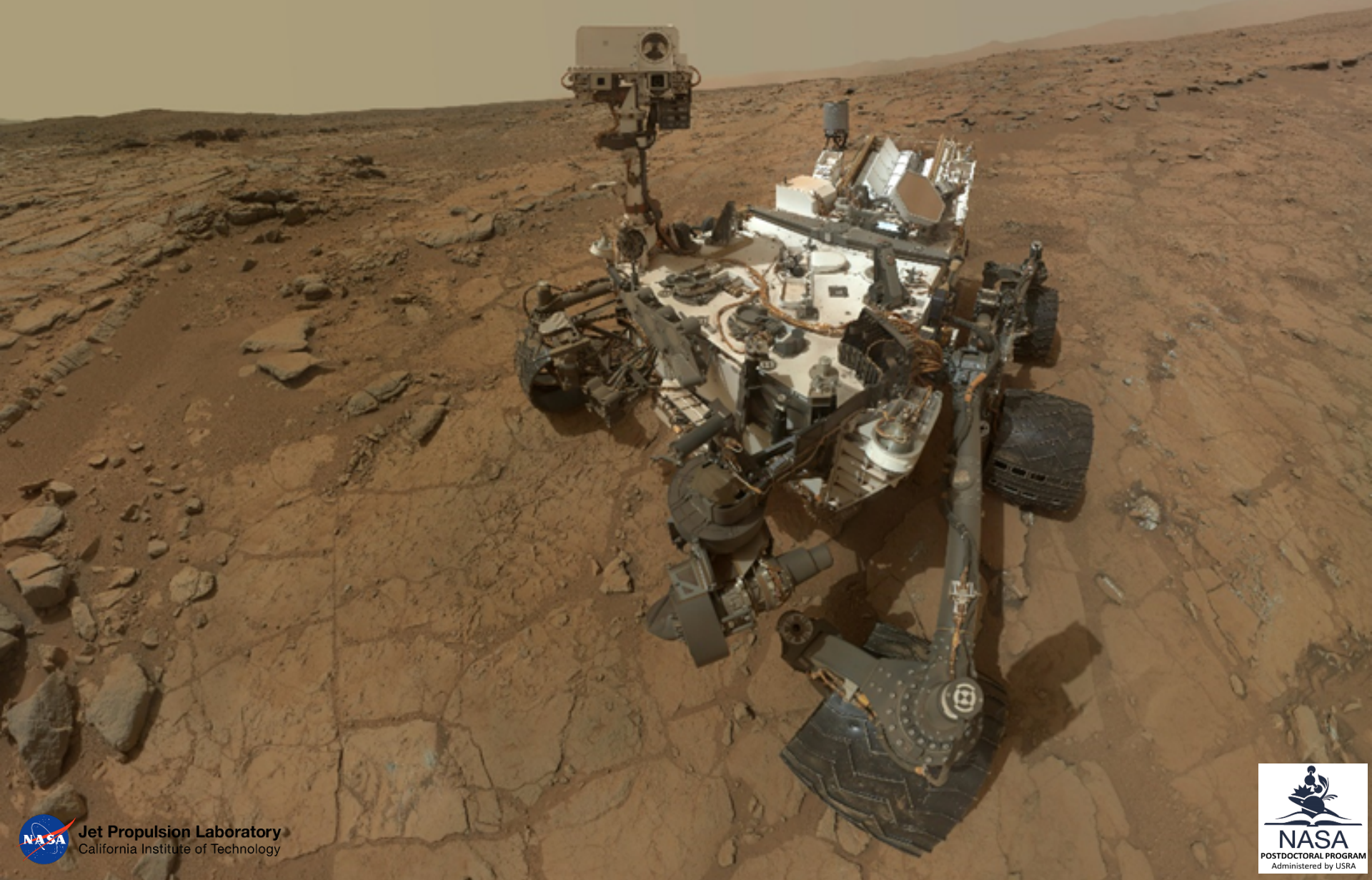
- This work was performed at the Jet Propulsion Laboratory (JPL), California Institute of Technology under a contract with the National Aeronautics and Space Administration (NASA)
- The work has been supported by the NASA Science Mission Directorate's Radioisotope Power Systems Program under the Thermoelectric Technology Development Project
- G. Cerretti's research at Jet Propulsion Laboratory was supported by an appointment to the NASA Postdoctoral Program, administered by Universities Space Research Association under contract with NASA.

Further information at:

- <https://rps.nasa.gov/>
- <https://www.jpl.nasa.gov/>
- **TECT Group, JPL**
- **Power and Sensors Systems Section, JPL**



**Jet Propulsion Laboratory**  
California Institute of Technology



**Jet Propulsion Laboratory**  
California Institute of Technology

